Molecular Biology of the Cell
Vol. 15, 3729–3739, August 2004

The Lipid Binding Pleckstrin Homology Domain in UNC-104 Kinesin is Necessary for Synaptic Vesicle Transport in *Caenorhabditis elegans*[D] [V]

Dieter R. Klopfenstein*† and Ronald D. Vale*‡§

*Department of Cellular and Molecular Pharmacology and ‡The Howard Hughes Medical Institute, University of California San Francisco, San Francisco, California 94143

Submitted April 21, 2004; Revised May 12, 2004; Accepted May 13, 2004
Monitoring Editor: Lawrence Goldstein

UNC-104 (KIF1A) is a kinesin motor that transports synaptic vesicles from the neuronal cell body to the terminal. Previous in vitro studies have shown that a *Dictyostelium* relative of UNC-104 transports liposomes containing acidic phospholipids, but whether this interaction is needed for the recognition and transport of synaptic vesicles in metazoans remains unexplored. Here, we have introduced mutations in the nonmotor domain of UNC-104 and examined whether these mutant motors can rescue an *unc-104 Caenorhabditis elegans* strain. We show that a pleckstrin homology (PH) domain in UNC-104 is essential for membrane transport in living *C. elegans*, that this PH domain binds specifically to phosphatidylinositol-4,5-bisphosphate ($PI(4,5)P_2$), and that point mutants in the PH domain that interfere with $PI(4,5)P_2$ binding in vitro also interfere with UNC-104 function in vivo. Several other lipid-binding modules could not effectively substitute for the UNC-104 PH domain in this in vivo assay. Real time imaging also revealed that a lipid-binding point mutation in the PH domain reduced movement velocity and processivity of individual UNC-104::GFP punctae in neurites. These results reveal a critical role for $PI(4,5)P_2$ binding in UNC-104–mediated axonal transport and shows that the cargo-binding properties of the distal PH domain can affect motor output.

INTRODUCTION

Neurons represent a specialized cell type that is particularly dependent on motor-driven transport in order to move membranes, protein complexes, and mRNA over large distances from the cell body to the tips of axons and dendritic arbors. Two types of microtubule-based motor proteins power membrane transport in neurons and other cells: kinesins, the majority of which move toward the plus ends of microtubules and the minus-end–directed motor cytoplasmic dynein (Hirokawa *et al.*, 1998; Vale, 2003). Kinesins are characterized by a ~40-kDa motor domain that exhibits 20–60% amino acid sequence identity throughout the kinesin superfamily. The nonmotor "tail" domains of kinesins exhibit considerable diversity in terms of their length and sequence and are thought to mediate specific binding to cargo and, in some cases, regulation of the motor activity. It therefore is not surprising that many cargo-transporting kinesins are expressed in the nervous system, some of them exclusively (Miki *et al.*, 2001). Mutations in neuronal kinesin genes recently have been linked to human neurodegenerative diseases, most likely as the consequence of impaired axonal transport (Zhao *et al.*, 2001; Reid *et al.*, 2002). Thus, understanding how neuronal kinesins recognize and transport cargo has become an important question for both cell biology and human disease.

The UNC-104/KIF1 kinesins represent an important class of cargo-transporting motors in the nervous system. The founding member of this class (UNC-104) was discovered in a genetic screen in *Caenorhabditis elegans* that yielded paralyzed or uncoordinated phenotypes (Hall and Hedgecock, 1991). In the case of Unc-104, this phenotype results from an accumulation of presynaptic vesicles in the cell body with reduced numbers of synaptic vesicles at nerve endings (Hall and Hedgecock, 1991; Otsuka *et al.*, 1991). *unc-104* mutant worms possess a normal neuronal anatomy and are viable, arguing for a specific function of this kinesin motor in membrane transport. An UNC-104–like kinesin (KIF1A) was later identified in mouse (Okada *et al.*, 1995), and a knockout of this motor yielded a similar presynaptic vesicle transport defect and resulted in death shortly after birth (Yonekawa *et al.*, 1998). A close UNC-104/KIF1A relative exists in *Dictyostelium*, and gene knockout experiments have shown that it serves as a vesicle transporter (Pollock *et al.*, 1999). This result indicates that the membrane transport capability of the Unc104/KIF1 motor class evolved in unicellular organisms.

To facilitate long range transport, UNC-104/KIF1A motors are the fastest among the animal kinesins (moving at 2–3-fold faster rates than conventional kinesin), and the mechanism of motility has been the subject of several structural and single molecule investigations (Okada and Hirokawa, 1999, 2000; Pierce *et al.*, 1999; Tomishige *et al.*, 2002; Okada *et al.*, 2003). In comparison with these numerous biophysical investigations, relatively little effort has been directed toward understanding how UNC-104 transports membranes. We have previously shown that *Dictyostelium*

Article published online ahead of print. Mol. Biol. Cell 10.1091/mbc.E04–04–0326. Article and publication date are available at www.molbiolcell.org/cgi/doi/10.1091/mbc.E04–04–0326.

[D] [V] Online version of this article contains supporting material. Online version is available at www.molbiolcell.org.

† Present address: DFG Research Center for Molecular Physiology of the Brain, Georg August University, Humboldtallee 23, 37073 Göttingen, Germany.

§ Corresponding author. E-mail address: vale@cmp.ucsf.edu.

Abbreviations used: $PI(4,5)P_2$, phosphatidylinositol-4,5-bisphosphate.

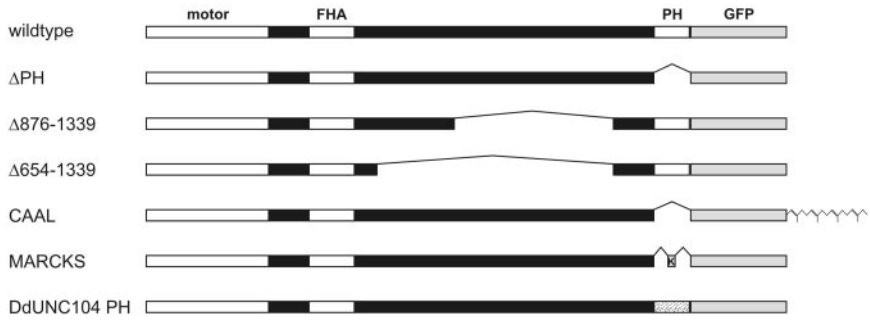

Figure 1. UNC-104 domain organization and tail domain deletion/substitution mutations. A schematic representation drawn to scale of UNC-104's domain structure is shown on top (from left to right): an amino-terminal motor domain (aa 1–348), a forkhead-homology (FHA) domain (aa 463–592), and elongated stalk region of unknown structure, and a C-terminal pleckstrin homology (PH) domain (aa 1460–1560). The green fluorescence protein was added at the carboxy-terminus. Constructs were created with either deletions of the PH domain (PH) or region between the motor and PH domains (878-1339, 654-1339) or substitutions of the PH domain with other lipid-binding domains (MARCKS basic domain, DdUnc104 PH; see MATERIAL AND METHODS for exact sequences used). The CAAL construct is based on the UNC-$104_{\Delta PH}$ constructs but has an isoprenylation consensus site (CAAL) at the C-terminus of the GFP.

UNC-104 can bind directly to acidic membrane lipids (most specifically to phosphatidylinositol-4,5-bisphosphate ($PI(4,5)P_2$)) through a C-terminal pleckstrin homology (PH) domain (Klopfenstein *et al.*, 2002). Moreover, the clustering of $PI(4,5)P_2$ lipids through the formation of lipid "raft" microdomains stimulated UNC-104–mediated transport of liposomes in an in vitro assay (Klopfenstein *et al.*, 2002). This potential motor-lipid interaction distinguishes the UNC-104 cargo-binding mechanism from other kinesin motors, whose identified tail domain–binding partners are either integral membrane proteins or soluble scaffolding proteins (Muresan, 2000). However, the physiological relevance of the UNC-104-lipid interaction remains in question, because the previous studies were performed using in vitro transport systems.

Here, we have tested the in vivo relevance of the PH domain and lipid interactions for UNC-104–mediated membrane transport in the nervous system of *C. elegans*. A major advantage of this system is that the uncoordinated, nearly paralyzed phenotype of *unc-104(e1265)* animals can be rescued by introducing a wild-type UNC-104 construct into this severe hypomorph (Zhou *et al.*, 2001). This rescue experiment offers the unique possibility of testing how mutations/deletions in the PH domain as well as other regions of UNC-104's nonmotor domain affect the ability of the motor to transport synaptic vesicle precursors in the nervous system of living *C. elegans*. We show that an UNC-104 motor lacking its C-terminal PH domain is unable to rescue the severe defects in vesicle transport and worm movement that characterize the *unc-104(e1265)* phenotype. We also demonstrate that the UNC-104 PH domain binds with high specificity to PI(4,5)P2 and that point mutations that reduce PI(4,5)P2 binding in vitro cause behavioral and vesicle transport defects in vivo. This study illustrates the physiological importance of motor-lipid interactions in membrane transport and constitutes the first in vivo structure-function analysis of a kinesin-cargo interaction.

MATERIALS AND METHODS

Materials

The following lipids were purchased from Avanti Polar lipids (Birmingham, AL): egg PC (Cat. no. 840051), PI(4)P (no. 840045), $PI(4,5)P_2$ (no. 840046), and PA (no. 840101); PI(3)P (no. 1773) and $PI(3,4,5)P_3$ (no. 1775) were from Matreya Inc. (State College, PA).

Constructs and C. elegans *Strains*

The full-length wild-type unc-104::GFP construct was kindly provided by Drs. Mimi Zhou and Jon Scholey (UC Davis; Zhou *et al.*, 2001). This plasmid was derived from the pPD95.77 vector (Drs. Si-Qun Xu and Andy Fire) containing the unc-104 promotor region (3.7-kb sequence upstream from the first exon) up to exon 5 from cosmid C47A5 and the genomic unc-104 exon/intron structure from exons 5–10 (from cosmid C52E12) fused to a cDNA consisting of exon 10–22. Mutations and deletions were introduced using standard PCR and DNA cloning techniques. Deletions between the motor domain and the PH domain were performed by replacing the original fragment between *Kas*I (position 8083) and *Bsp*EI (position 10892) with a PCR fragment of desired length (deletions of aa 461-1339, 654-1339, 878-1339). Deletions (Δ461–1339, Δ654–1339, Δ878–1339) and point mutations (KK1463/4AA, RR1479/80AA, RR1485/6AA, R1496A, K1522A, R1534A) in the PH domain were performed by replacing the original *Bsp*EI/*Knp*I fragment (nucleotides 10892–11743) with PCR products of desired deletion and mutations (Figure 1). Point mutations were prepared using a QuickChange mutagenesis kit (Stratagene, La Jolla, CA). In constructs with a substituted PH domain, the UNC-104 PH domain (aa 1460–1560) was replaced by the following sequences: MARCKS basic domain (Wang *et al.*, 2002; aa 151–175; (CKKKKRFSFKKSFKLSGFSFKKNKK)), the PH domain of DdUnc104 (Pollock *et al.*, 1999; aa 1518–1625), or the PH domain of rat PLCδ1 (Kavran, 1998; no. 70; aa 30–132). For the liposome binding assays, the UNC-104 motor domain (aa 1–446) was joined to the PH domain (aa 1449–1584) in an *Escherichia coli* pET17b expression vector (Novagen, Madison, WI). All constructs were verified by DNA sequencing.

All *C. elegans* strains for analysis were derived from the *unc-104* line (CB1265 [unc-104(e1265) II] and maintained at 20–25°C using standard methods (Brenner, 1974). Heritable lines of transgenic worms carrying extrachromosomal arrays of the UNC-104::GFP construct (Zhou *et al.*, 2001) were created by microinjecting the UNC-104::GFP plasmid (70 μg/ml) into *unc-104(e1265)* hermaphrodites by methods described previously (Fire, 1986; Mello *et al.*, 1991). Extrachromosomal arrays had the following designations: UNC-104_{wt}, pjEx8-1; UNC-$104_{\Delta PH}$, pjEx21-2; UNC-$104_{\Delta 654-1339}$, pjEx26-5; UNC-$104_{\Delta 878-1339}$, pjEx49-1; UNC-104_{CAAL}, pjEx12-1; UNC-104_{MARCKS}, pjEx66-5; UNC-104_{DdPH}, pjEx35-3; UNC-$104_{KK1463/4AA}$, pjEx113-1; UNC-$104_{RR1479/80AA}$, pjEx116-3; UNC-$104_{RR1485/6AA}$, pjEx85-2; UNC-104_{R1496A}, pjEx99-1; UNC-104_{K1522A}, pjEx110-1; UNC-104_{K1534A}, pjEx108-1. Transgenic lines were selected on the basis of either their sinusoidal, wild-type movement and/or GFP expression as examined using a Leica MZFLIII microscope (Leica Microsystems, Bannockburn, IL). Locomotion was assayed by touching the head or tail of the worm with an eyelash to stimulate backward or forward movement.

Worm Motility Assays

Young adult hermaphrodite velocities were assayed after transferring well-fed, M9-buffer washed worms onto a fresh NGM agar plate without food and allowing them to accommodate for 1 h. Movement was recorded on a Wild M3Z dissecting microscope at 160× magnification at 1–3 frames per sec (640 × 480 pixels) for 3–10 min with a Javelin CC TV camera (Torrance, CA) and Adobe Premiere 4.0 (San Jose, CA). Movements were tracked using a custom programmed ImageJ's multitracker plugin (NIH, ImageJ version 1.30; Nico Stuurman, UCSF). A blurred image of the first image in the stack was made (Gaussian blur, radius 5 pixels) and subtracted from the entire stack to reduce the background for conversion into a threshold stack. The centroid position of adult worms with an apparent pixel size of 60–200 and a minimal tracking length of 15 frames was tracked. Worm velocity was calculated in a spreadsheet program by calculating the straight line distance between centroid positions in a 3-s interval. The directionality of movement was measured by calculating the trajectory angle of the centroid position over a 3-s interval relative to an arbitrary vertical line (0°). Worm track images on agar plates were taken on a Nikon dissecting microscope with a Nikon Coolpix5000 digital camera at full resolution (Garden City, NY).

Bacterial Protein Expression and Purification

The PH domain and flanking regions (aa 1442–1584) of UNC-104 was cloned using standard PCR into a modified pET17b vector (Novagen) with a 5′ flanking UNC-104 motor domain (aa 1–446) and with a 3′ flanking His_6 extension following the C-terminal PH domain residue. Lysines and arginines in the PH domain were mutated using QuickChange mutagenesis (Stratagene). All constructs were verified by DNA sequencing. Proteins were expressed and purified by Ni-NTA chromatography (QIAGEN, Valencia, CA) followed by HiTrap-Q or HiTrap-S ion exchange chromatography (Amersham Pharmacia Biotech, Piscataway, NJ). Motors were either assayed or were frozen with 10% sucrose added and stored in liquid nitrogen.

Membrane Floatation Assay

Liposomes were prepared as previously described (Klopfenstein *et al.*, 2002). The membrane floatation was performed as follows: liposomes (100 μl of 10 mM total lipid concentration) were incubated on ice for 30 min with 1.5 μg mini-motor. LB buffer (30 mM Tris, 4 mM EGTA, 2 M sucrose, pH 8.0) was added to the incubation reaction to bring the final sucrose concentration to 1.6 M, and this mixture was overlaid with cushions containing 1.4 M, 0.4 M, and 0.25 M sucrose in the same buffer in a TLS-55 tube. After centrifugation at 201,000 $\times$ *g* (4°C) for 30 min in a TLS-55 rotor (Beckman, Fullerton, CA), the 0.25/0.4 M interphase (top fraction), 0.4 M/1.4 M interphase (middle fraction), and the loading fractions were collected and analyzed by SDS-PAGE followed by Coomassie-stained analysis. Gels were digitized by flatbed scanning, and protein bands were quantified using ImageJ 1.30 software (NIH, Bethesda, MD).

Primary Neuronal Cell Culture

Primary cell culture was performed according to Christensen *et al.* (2002). In brief, embryonic cells were prepared by treating synchronized adult nematodes with an alkaline hypochlorite solution (0.5 M NaOH and 1% NaOCl) for 5 min. Eggs released by this treatment were collected by centrifugation and then washed three times with egg buffer containing 118 mM NaCl, 48 mM KCl, 2 mM $CaCl_2$, 2 mM $MgCl_2$, and 25 mM HEPES, pH 7.3. Adult carcasses were separated from washed eggs by density centrifugation in 30% sucrose. The egg layer was removed by pipette and washed one time with egg buffer and then pelleted. Eggshells were removed by resuspending pelleted eggs in egg buffer containing 1–2.5 U/ml chitinase for 45–90 min at room temperature. After digestion of the eggshell, the suspension was gently pipetted up and down several times to dissociate the cells. Cells were washed twice with L-15 cell culture medium (Life Technologies, Rockville, MD) containing 10% fetal bovine serum (Hyclone, Logan, UT), 50 U/ml penicillin, and 50 μg/ml streptomycin and adjusted to 345 mOsm with sucrose. Dissociated embryo cells were filtered through a sterile 5-mm Durapore syringe filter (Millipore, Billerica, MA) to remove undissociated embryos and newly hatched larvae. Filtered cells were plated on 14-mm-diameter glass-bottomed cell culture dishes (MatTek, Ashland, MA) coated with 0.5 mg/ml peanut lectin agglutinin (Sigma, St. Louis, MO). Cultures were maintained at 24°C in a humidified incubator in L-15 cell culture medium.

Microscopy and Immunofluorescence

Fixed animals were immunostained with antisynaptotagmin (Nonet *et al.*, 1993) antibodies as described (Finney and Ruvkun, 1990). Images were taken on a Zeiss Axiovert 200M (Thornwood, NY) with a cooled CCD camera (SensiCam; Cooke Camera, Auburn Hill, MI) or for live imaging on a QLC100 spinning disk head with a Stanford Photonics XR MEGA10 camera (Palo Alto, CA) attached to the Zeiss Axiovert 200M microscope. For live cell imaging, images were acquired at 2–3 frames per sec. Images were analyzed using ImageJ 1.30 software (NIH). A line was drawn over the neurite of interest, and the reslice stack function was used to obtain a kymograph image of that line as a function of time. Particles appear as lines; for a moving particle, this line is oblique and its slope corresponds to the velocity of the particle. The lines obtained for stationary particles were used to correct for movement of the stage. Velocities were calculated for periods of unidirectional movement toward the neurite growth cone.

RESULTS

The PH Domain Is Required for UNC-104–mediated Transport In Vivo

Previous studies demonstrated that the nearly paralyzed body movement of *unc-104(e1265)* hypomorph worms can be fully restored to wild-type movement by microinjecting a plasmid expressing the full-length UNC-104 motor (Zhou *et al.*, 2001). This finding provided the starting point for our work to test the in vivo cargo transport activity of mutant UNC-104 proteins. *unc-104(e1265)* worms exhibit a reduction in vesicle transport, leading to a retention of presynaptic vesicles in the soma with fewer vesicles localized at the synapse and as a consequence show uncoordinated body movement due to reduced synaptic transmission. We first repeated the transgenic rescue experiment of Zhou *et al.* (2001) by introducing wild-type UNC-104::GFP into *unc-104(e1265)* animals. The motor was expressed in motor and sensory neurons using the endogenous unc-104 promoter to ensure appropriate expression levels and rescue of phenotype. At least five transgenic worm lines were propagated for each construct described in this article, and in all cases, the results were similar for the different isolates. In addition, all transgenic animals described in this article expressed comparable levels of UNC-104::GFP as assessed by fluorescence in the nervous system, indicating that the phenotypes described here cannot be explained by a failure in expression or protein folding defects leading to degradation.

To analyze transgenic animals, we performed time-lapse microscopy of the worms on agar plates and developed algorithms that tracked the worms' centroid position and analyzed the velocity and directional persistence of movement (see MATERIAL AND METHODS). Transgenic *unc-104* animals expressing the wild-type UNC-104 motor displayed rapid movement across the plate (12.7 $\pm$ 3.6 mm/min; mean $\pm$ SD), whereas the *unc-104* animals exhibited very slow velocities (1.1 $\pm$ 0.9 mm/min; Figures 2 and 3A; Table 1). The tracks on the agar plate made by animals expressing wild-type UNC-104 reveal coordinated movement characterized by a regular, sinusoidal pattern of tracks on the agar plate (Figure 2). In contrast, tracks made by *unc-104* animals show an irregular pattern, indicating a lack of coordinated movement (Figure 2). To determine the persistence of movement, we plotted the direction of movement starting at the center of a polar diagram (time = 0 and the initial angle arbitrarily set at 0°) and moving outwards over time (Figure 3B). The transgenic worms expressing the wild-type motor tended to move persistently in a given direction (Figure 3B), although abrupt transitions in direction occurred (see Supplementary Figure 1 for additional traces). In contrast, the *unc-104* animals failed to show persistent, unidirectional motion, as evidenced by the spread of points over the polar diagram (Figure 3B).

Next, we examined the role of the PH domain in UNC-104–mediated axonal transport, because our previous studies showed that this domain was necessary for membrane transport in vitro by the *Dictyostelium* Unc104 motor (Klopfenstein *et al.*, 2002). We created transgenic worms, in the *unc-104* background (e1265), that expressed an UNC-104 motor bearing a deletion of the canonical PH domain (termed UNC-$104_{\Delta PH}$). Transgenic worms expressing (UNC-$104_{\Delta PH}$) behaved very similar to *unc-104* animals in their movement velocity (0.9 $\pm$ 1.0 mm/min), the uncoordinated appearance of the worm tracks, and the lack of persistent, unidirectional motion (Figures 2 and 3B; Supplementary Figure 1). These results indicate that the PH domain is essential for UNC-104 function in the *C. elegans* nervous system.

unc-104 worms show a 60% reduction in the number of presynaptic vesicles localized at the synapse compared with wild-type animals (Hall and Hedgecock, 1991) and an accumulation of these synaptic vesicle precursors in the cell body (Nonet *et al.*, 1993). To determine if the phenotype of the UNC-$104_{\Delta PH}$-expressing worms similarly might be explained by reduced transport efficiency of synaptic vesicles, we examined the distribution of synaptotagmin (a synaptic vesicle marker) by immunofluorescence in whole animals (Nonet *et al.*, 1993). In the animals expressing wild-type UNC-104, the synaptic vesicle staining was found through-

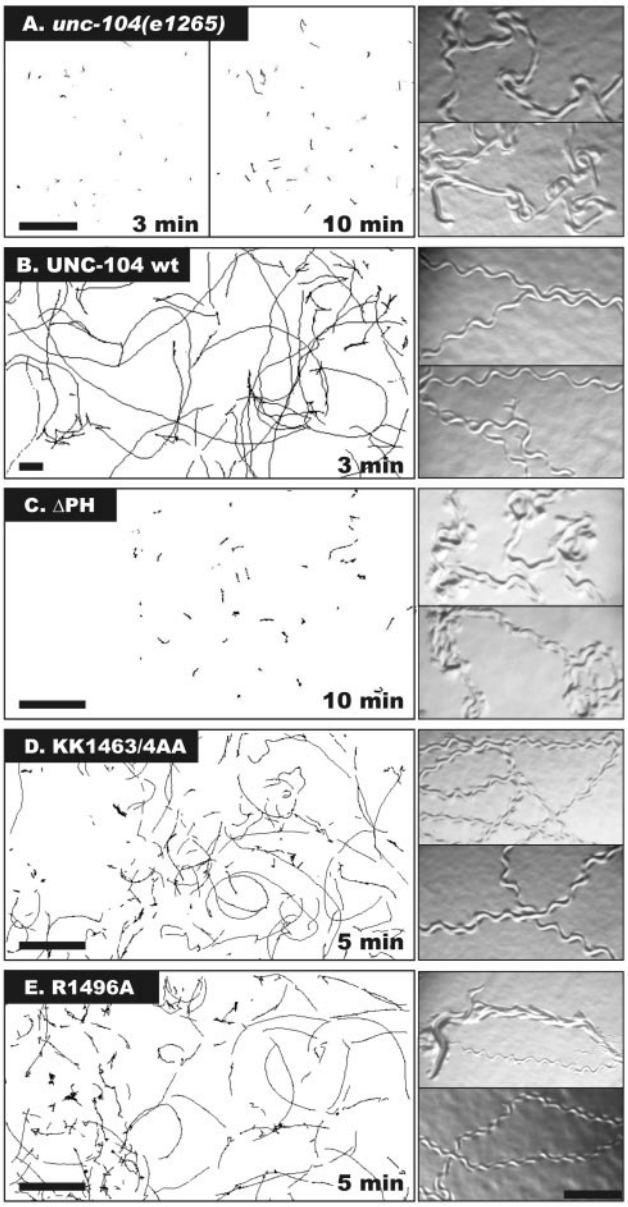

Figure 2. The effects of PH domain deletion and point mutations on the ability of UNC-104 constructs to rescue worm movement. Left panels: The movement of *unc104(e1265)* worms or *unc-104* animals expressing wild-type (wt) UNC-104, or UNC-104 with a deletion of either the PH domain (ΔPH) or the PH domain point mutations KK1463/4AA or R1496A. Young adult worms were placed on agar plates, and their position was recorded over an interval of either 3 min (wt), 5 min (KK1463/4AA, R1496A), or 10 min (*e1265*, ΔPH). The motion was tracked using a computer algorithm (MATERIAL AND METHODS). Scale bar, 4 mm. Right panels: Worm tracks on a bacterial lawn reveal the degree of coordination. *unc-104* worms show coordinated movement, but expression of wt UNC-104 restores coordinated motion, as seen in the regular sinusoidal pattern of the tracks. The UNC-$104_{\Delta PH}$–expressing worms behave similar to the *unc-104* animals, and the UNC-$104_{KK1463/4AA}$ or UNC-104_{R1496A}–expressing animals display decreased velocities compared with wild type. Scale bar, 0.3 mm.

out the axonal processes within ventral nerve cord of *C. elegans* (diffuse staining along the nerve in Figure 4). In contrast, in the *unc-104* and UNC-$104_{\Delta PH}$–expressing animals, synaptotagmin staining accumulated in the cell bodies of sublateral neurons, and there was a significant reduction in staining in the ventral nerve cord (Figure 4).

We also prepared primary neuronal cell cultures from transgenic animals expressing wild-type or mutant UNC-104 (Christensen *et al.*, 2002). For neurons in culture expressing wild-type motor, synaptotagmin staining was observed in the cell body, neurites, and nerve terminals. In the cultured neurons derived from the *unc-104* and UNC-$104_{\Delta PH}$–expressing animals, the staining was mostly confined to the cell body, although some staining was observed in the neurite (Figure 4; quantitation in Supplementary Figure 3). Notably, the *unc-104* and UNC-$104_{\Delta PH}$–expressing neurons did not show concentrated synaptotagmin staining at the neurite tips, which was observed in about half of the cells expressing wild-type UNC-104. Therefore, the uncoordinated phenotype of *C. elegans* expressing the UNC-$104_{\Delta PH}$ motor can be explained by the failure to properly localize synaptic vesicles.

Point Mutations in the PH Domain That Reduce PI(4,5)P_2 Binding In Vitro Also Cause Phenotypic Defects In Vivo

We next wanted to determine whether the *C. elegans* UNC-104 PH domain has lipid-binding activity and, if so, whether its lipid-binding activity is important for axonal transport. For testing lipid-binding activity, a recombinant *C. elegans* mini-motor construct was created in which the PH domain was joined after the FHA domain and analyzed for binding to liposomes prepared with various lipid compositions (MATERIAL AND METHODS). The PH domain-containing mini-motor bound preferentially to liposomes composed of 10% PI(4,5)P_2/90% phosphatidyl choline (PC) compared with other phosphoinositide or acidic phospholipids; little binding to liposomes composed solely of PC was observed (Figure 5B). Thus, the *C. elegans* UNC-104 PH domain, like the PH domain of the *Dictyostelium* Unc104 motor (Klopfenstein *et al.*, 2002) displays specific phosphoinositide lipid recognition.

We next sought to identify point mutations in the *C. elegans* PH domain that reduce PI(4,5)P_2 binding in vitro. To identify candidate lysine and arginine residues that might be involved in binding to acidic phospholipid head groups (Lemmon and Ferguson, 2001; Lemmon, 2003), we aligned the sequences of UNC-104 PH domains from several species (Figure 5A). On the basis of this alignment, we created five mutations in which single or pairs of conserved basic residues were changed to alanine, and these mutant proteins were tested for binding to PI(4,5)P_2-containing liposomes in vitro. Of the five proteins tested, only the KK1463/4AA and R1496A mutations affected liposome binding, both reducing binding by ~70% (Figure 5C).

We prepared transgenic worms expressing full-length UNC-104::GFP motors bearing the six PH domain mutations that were analyzed in vitro. Three of the mutations (RR1479/80AA and R1534A, Supplementary Figure 2; and RR1485/6AA, unpublished data) that had no effect on lipid-binding in vitro produced a full rescue of worm motility (Table 1). The third mutation (K1522A) that did not alter lipid binding in vitro, however, did not fully restore worm motility (approximately one-fifth the velocity of wild type) although the worms exhibited directional motion (Table 1; Supplementary Figure 2). The reason for this phenotypic defect is not clear, although it is possible that the mutation of this highly conserved residue affected a function of the PH domain other than lipid binding.

The two PH mutations that reduced lipid binding by 70% in vitro also produced phenotypic defects in vivo (Figure 2

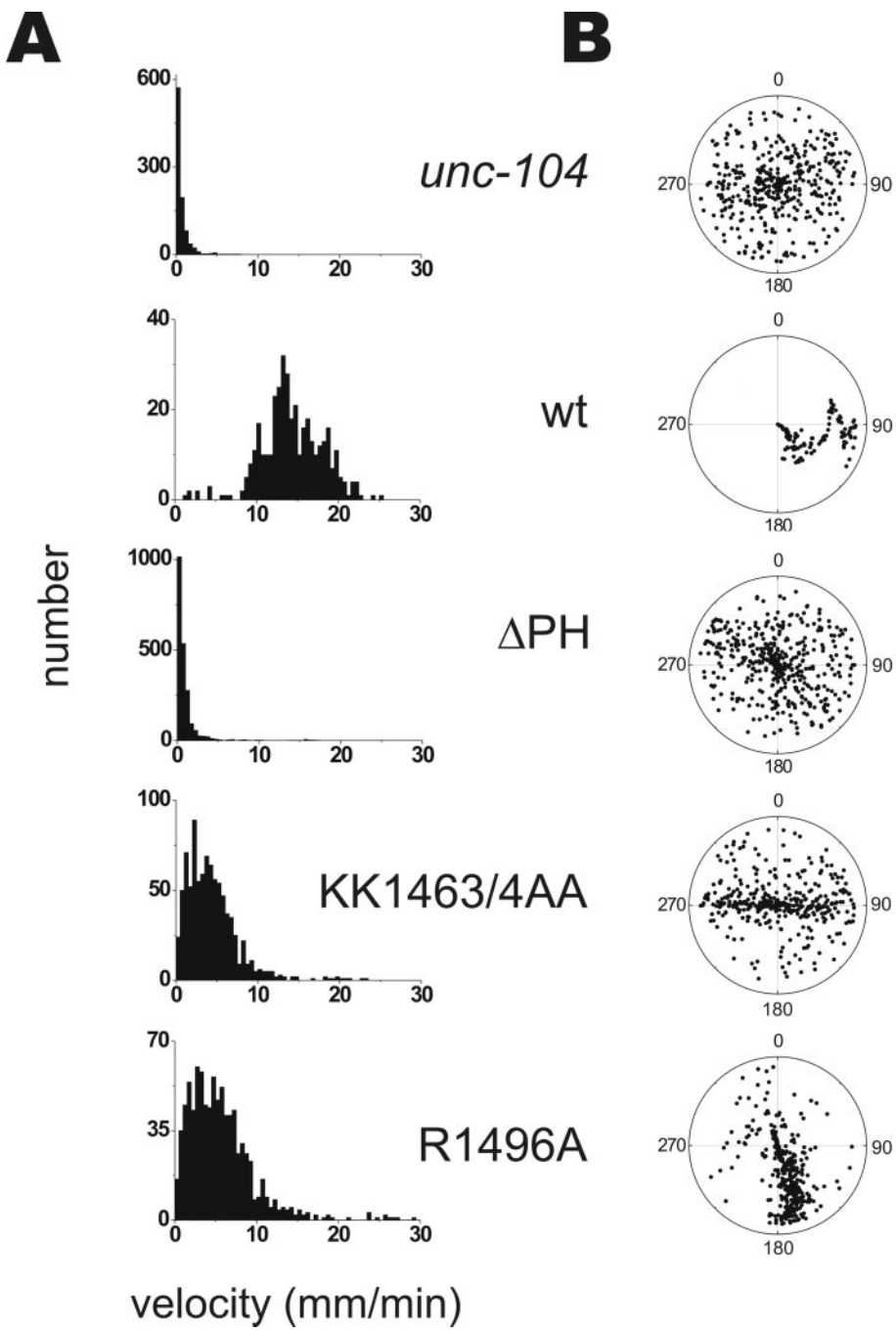

Figure 3. Analysis of worm velocity and directional persistence. (A) Worm tracks were analyzed by measuring the displacement >3-s intervals, and the resultant velocities from five animals were compiled and plotted as histograms. The mean velocities and standard deviations are shown in Table 1. UNC-104 wild-type animals show a broad range of velocities and only occasional pauses, whereas *unc-104* and ΔPH animals spend most of their time in a very slow moving state (left bin of the histogram). (B) The directionality of movement of single worms was analyzed in this polar plot. The worm starts at the center of the plot (time 0, angle arbitrarily set at 0° parallel to the long axis of the animal) and at each second, the angle in which the worm is moving is plotted. The *unc-104* animals do not show persistent motion, as indicated by the spread of points throughout the polar plot; similar results are true for UNC-104$_{\Delta PH}$–expressing animals. On the other hand, wt UNC-104, UNC-104$_{R1496A}$, and UNC-104$_{KK1463/4AA}$–expressing animals often exhibited persistent motion, but the later sometimes showed frequent backwards and forwards motion. Additional directionality plots are found in Supplementary Figure 1.

and Table 1). UNC-104$_{KK1463/4AA}$ and UNC-104$_{R1496A}$–expressing worms moved more slowly (3.6 ± 3.0 and 4.3 ± 3.0 mm/min, respectively) than wild-type animals. The tracks revealed sinusoidal movement, but not with the same regular characteristics as wild-type, and the worms often failed to show persistent unidirectional motion (Figures 2 and 3). Consistent with this phenotypic defect, immunofluorescence showed synaptotagmin accumulation in cell bodies in the ventral nerve cord, which was rarely seen with wild-type UNC-104 (Figure 4). The R1496A mutant caused a partial accumulation of synaptotagmin staining in the sublateral neuronal cell bodies, but these worms could still transport this synaptic vesicle marker efficiently into the axons of the ventral nerve cord (Figure 4). For neurons in culture (bottom panel), the KK1463/4AA showed some accumulation of synaptotagmin in the cell body, whereas the R1496A mutant was comparable to wild-type UNC-104 neurons using this cell culture assay (Figure 4, quantitation in Supplementary Figure 3).

We also sought to directly track UNC-104::GFP motion in neurons from animals expressing wild-type UNC-104 or the lipid-binding UNC-104$_{R1496A}$. Zhou *et al.* (2001) were able to image directional motion of UNC-104::GFP (presumably bound to membranes) in axons of transgenic animals in situ. We were able to observe a few examples of linear movement of UNC-104::GFP in worms as well. However, our background of soluble UNC-104::GFP was sufficiently high, especially in the thick specimen of the

Table 1. Velocities of *unc-104(e1265)* animals or *unc-104* animals expressing wt UNC-104 or UNC-104 motors bearing the indicated deletions, PH domain substitutions, or PH domain point mutations

Construct	Velocity (mm/min)	SD	n
unc-104(e1265)	1.1	0.9	150
wt	12.7	3.6	454
ΔPH	0.9	1.0	772
CAAL	2.3	1.6	268
Δ878–1339	2.4	0.7	313
Δ654–1339	1.7	1.0	134
KK1463/4AA	3.6	3.0	183
R1496A	4.3	2.2	322
RR1479/80AA	13.2	3.7	374
K1522A	2.2	1.6	61
MARCKS	1.2	1.1	105
DdUnc104PH	0.9	1.2	69

Average worm velocities are expressed in mm/min ± SD with the number of worms analyzed (n). In comparison, N2 wild-type worms move at a velocity of 13.4 ± 4.5 mm/min (n = 85). Numbers are derived from at least two independent experiments. The velocities of ΔPH, MARCKS. DdUnc104PH, was not statistically different from the *unc-104* animals ($p > 0.001$), but the other constructs were statistically different ($p < 0.001$).

whole worm, to preclude clear imaging of the subset of motors bound to small, moving vesicles, at least with our imaging system.

We next attempted to image motion of cultured neurons derived from UNC-104::GFP-expressing animals, which provided a thinner preparation for imaging. Although the background of soluble UNC-104::GFP was still high, we could observe more frequent linear motions of UNC-104::GFP punctae in cultured neurons with a spinning disk confocal microscope (Supplementary Movie 1). Although identity of these punctae is not certain, we believe that they reflect several UNC-104::GFP motors bound to a membranous organelle. Movement of small membrane vesicles containing one or a few UNC-104::GFP motors are not likely to be scored, because the high background of soluble UNC-104::GFP would render them undetectable. Movement was generally directed toward the neurite growth cone, although short reversals of movement toward the cell body (presumably dynein-based) were observed. When movies were converted to kymographs (see MATERIAL AND METHODS), examples of linear UNC-104::GFP motion were evident (Figure 6). Analysis of these movements revealed a mean velocity of 0.8 ± 0.5 μm/s and a mean run length of 4.3 ± 2.1 μm. These velocities are similar to those described for UNC-104 by Zhou *et al.* (2001) and KIF1A by Lee *et al.* (2003). We also analyzed the movement of $UNC\text{-}104_{R1496A}$::GFP in cultured neurons. Linear movements of GFP particles were observed (Figure 6), but the analysis shows a statistically significant defect in velocity (0.43 ± 0.36 μm/s; $p < 10^{-7}$) and run length (2.5 ± 1.3 μm; $p < 10^{-7}$) compared with wild-type UNC-104::GFP. These results reveal the somewhat surprising outcome that a lipid-binding mutation in the distal UNC-104 PH domain affects the velocity and processivity of the motor in vivo. Possible explanations for this result will be presented in the DISCUSSION.

Substitution of the PH Domain with Other Lipid-binding Modules

Because our studies showed that the lipid-binding properties of the UNC-104 PH domain are important for axonal transport, we next tested the effects of substituting the PH domain with other lipid-binding domains: the PH domains from PLCδ1 and the *Dictyostelium* Unc104 (both specific for $PI(4,5)P_2$), the basic peptide domain from MARCKS, which has been shown to bind with high affinity and cluster $PI(4,5)P_2$ (Laux *et al.*, 2000; Wang *et al.*, 2002) and an C-terminal isoprenylation consensus site (CAAL). All of the above constructs generated transgenic animals, except for PLCδ1, which produced embryos that were positive for GFP expression but never hatched at any injected plasmid concentration (1–50 ng/μl). The reason for this dominant negative effect is not clear, but it precluded further analysis of this construct.

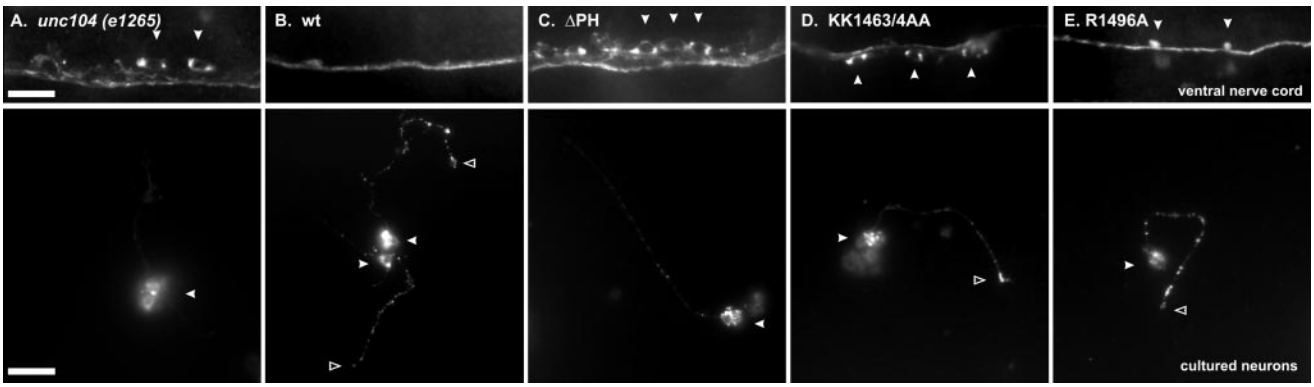

Figure 4. Synaptotagmin localization in *C. elegans* and in neurons in culture. Top: Synaptotagmin (a synaptic vesicle marker) localization in the ventral nerve cord of *unc104* (e1265) animals and in *unc-104* animals expressing wt UNC-104, $UNC\text{-}104_{\Delta PH}$, $UNC\text{-}104_{KK1463/4AA}$, or $UNC\text{-}104_{R1496A}$ motor proteins. In the *unc104* animals, the staining is mostly confined to neuronal cell bodies (examples indicated by arrows) with a weak staining in the axons running horizontally in the cord, indicating a failure to transport synaptic vesicles. On the other hand, animals expressing wt UNC-104 have robust axonal staining in the ventral nerve cord. The $UNC\text{-}104_{\Delta PH}$ and $UNC\text{-}104_{KK1463/4AA}$-expressing animals also show retention of synaptic vesicles in neuronal cell bodies (arrows). Scale bar, 10 μm. Bottom: Synaptotagmin localization in primary cell culture neurons derived from the worms shown on the left half. While wt UNC-104 and the point mutation–expressing animals show considerable staining in the neurites and often at neurite tips, the *unc104* and $UNC\text{-}104_{\Delta PH}$–expressing animals, on the other hand, tend to have decreased staining in the neurite (particularly at tips) but accumulated staining in the cell body. Cell bodies are indicated by arrows. Scale bar, 10 μm.

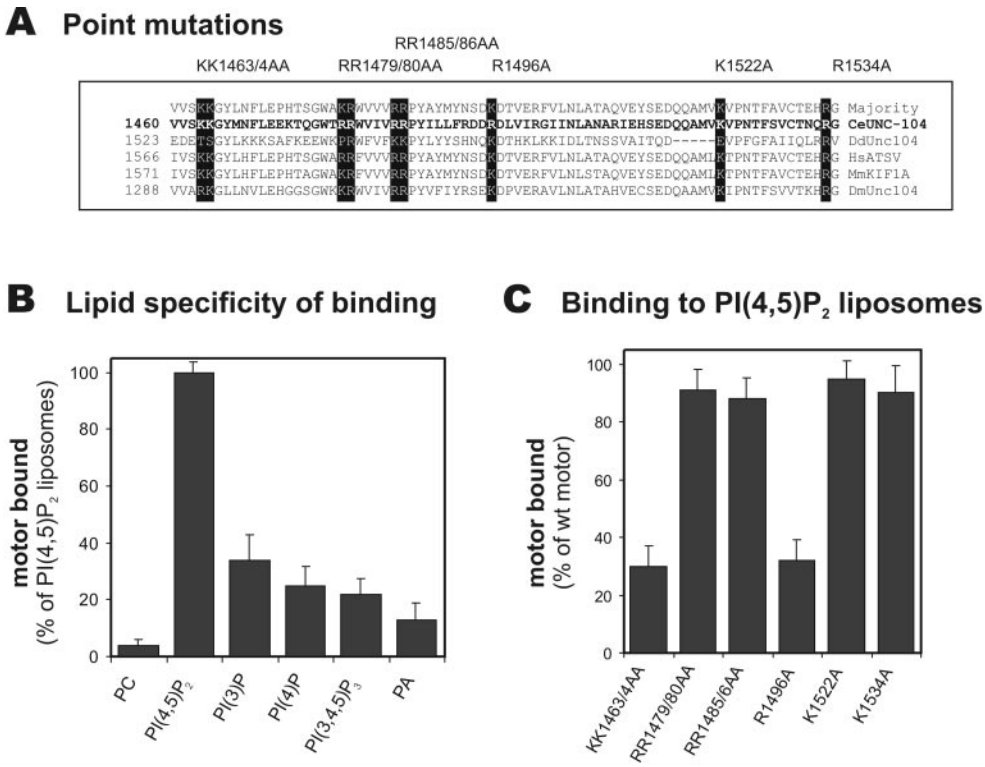

Figure 5. The UNC-104 PH domain binds selectively to PI(4,5)P_2 and point mutants in conserved basic residues reduce binding. Primary sequence alignment of the PH domains of UNC-104/KIF1A family members: *C. elegans* (CeUNC-104), *D. discoideum* (DdUnc104), *H. sapiens* (HsATSV), *M. musculus* (MmKIF1A), and *D. melanogaster* (DmUnc104). Conservation in positively charged amino acids in at least 4 of 5 members are highlighted. (B) A mini-UNC-104 consisting of the first 446 amino acids followed by the PH domain (1446–1584) was loaded at the bottom of a sucrose gradient together with liposomes containing either 100% phosphatidylcholine (PC) or 90% PC and 10% of the indicated phospholipids (PA, phosphatidic acid). After centrifugation in a step sucrose gradient to float liposomes, fractions from the top liposome layer and the bottom unbound layer were collected and analyzed by SDS-PAGE and Coomassie staining (see MATERIAL AND METHODS). The data were expressed as the % of the motor that bound to the 10% PI(4,5)P_2 liposomes. In this experiment, 40% of the added UNC-104 mini-motor (1.5 μM total) was bound to the 10% PI(4,5)P_2 liposomes. The mean and SD are shown for three experiments. (C) Effect of PH domain point mutations on PI(4,5)P_2 binding. Binding efficiency was calculated by comparing the specific binding values to PI(4,5)P_2 vs. PC liposomes, subtracting the corresponding nonspecific PC binding value from the PI(4,5)P_2 binding, and then expressing the ratio between wild-type and mutant PH domain constructs. The nonspecific binding of the point mutants to PC liposomes was similar to wild type. The mean and SD are shown for three experiments.

The PH domain substitutions UNC-104_{CAAL}, UNC-104_{MARCKS}, and UNC-104_{DdPH} exhibited either a weak or no rescue when compared with UNC-$104_{\Delta PH}$–expressing or *unc-104* animals (Figure **7**). The UNC-104_{CAAL}–expressing worms displayed improved velocity (2.3 $\pm$ 1.6 mm/min) and coordinated movement compared with *unc-104* animals; synaptotagmin staining showed accumulation within cell bodies of neurons in vivo and in culture, but was also observed in the axons of the ventral nerve cord, consistent with a partial rescue of UNC-104 transport function. These results suggest that a lipid anchor is sufficient for membrane interaction and a partial rescue of the uncoordinated phenotype. The overall average worm velocities of UNC-104_{MARCKS} and UNC-104_{DdPH} were not significantly different from *unc-104* animals (Table 1). However, the histograms show many UNC-104_{MARCKS} and UNC-104_{DdPH}–expressing animals moving $>$ 5 mm/min (Figure 7) in contrast to *unc-104* (Figure 3). None of these phenotypes are due to a dominant-negative effect caused by the PH domain substitution, because backcrossing these transgenetics with wild-type animals yielded progeny that displayed normal, coordinated movement (unpublished data). We also were unable to visualize movement of UNC-104::GFP bearing these lipid-binding domain substitutions in cultured neurons (unpublished data), although most likely short movements or movement of small organelles would have been missed by this technique. In conclusion, substitution of the UNC-104 PH domain with other lipid-binding modules can, at best, only weakly restore UNC-104 function in the nervous system.

DISCUSSION

Previously, we demonstrated that the PH domain of UNC-104 from the unicellular *Dictyostelium discoideum* binds to phosphoinositol-containing lipids and that this domain and its lipid-binding activity are important for reconstituting membrane transport in vitro. However, it remained possible that the conclusions from this in vitro system may not pertain to transport within a cell. In this study, we have explored the role of the PH domain and other regions of the UNC-104 tail domain for membrane transport in the physiological context of a living animal, the nematode *C. elegans*. This system has permitted structure-function studies of the motor cargo-binding domain, allowing us to examine and correlate the consequences of mutations on biochemical parameters (e.g., lipid binding), synaptic vesicle localization in neurons in situ and in culture, and whole animal behavior. Our studies show that the PH domain is essential for Unc104-mediated transport in vivo and provide strong evidence that the lipid-binding activity of this domain plays an important role in this activity.

Role for the PH domain and its Lipid Binding in UNC-104–mediated Transport

The phenotype of worms expressing UNC-$104_{\Delta PH}$ was nearly as pronounced as that from *unc-104* animals, indicating that the PH domain is a critical cargo-binding element of the motor. Moreover, we found that two PH domain mutations (R1496A and KK1463/4AA) that showed reduced binding to PI(4,5)P_2 also impaired the ability of expressed UNC-104 to rescue the *unc-104* uncoordinated phenotype.

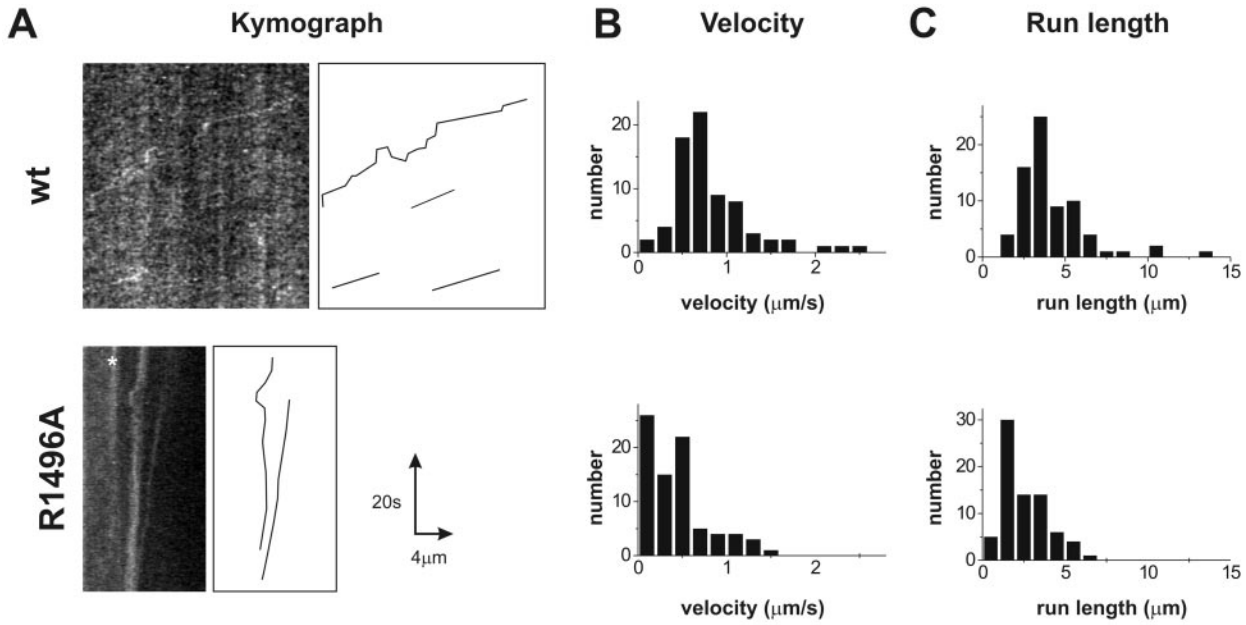

Figure 6. Tracking of movement of UNC-104::GFP in cultured neurons using live cell fluorescence imaging. (A) Kymographs of cultured neurons from *unc-104* worms expressing UNC-104_{wt} (top) or UNC-104_{R1496A} (bottom). A straight line was drawn over an extended neurite along which the fluorescence intensity was recorded in each frame the image stack. Persistent movement of UNC-104::GFP particles appear as straight lines from which the velocity and run length are calculated. Particle movement in the images (left) are manually traced and shown in the diagram on the right. (B) Histogram of velocity distribution of fluorescent particles movement in UNC-104_{wt} neurons (top) and UNC-104_{R1496A} (bottom). A significantly different mean velocity of 0.82 ± 0.45 μm/s (UNC-104wt) from 0.43 ± 0.36 μm/s (UNC-104_{R1496A}) was measured ($p < 10^{-7}$). (C) Histogram of run length distribution of fluorescent particles show a significantly longer mean run length for UNC-104_{wt} particles (top, 4.3 ± 2.1 μm) than for UNC-104_{R1496A} (bottom, 2.5 ± 1.3 μm, $p < 10^{-7}$). Note that because of technical limitations, short run lengths were difficult to measure and thus the histogram does not follow an exponential curve. Numbers reflect mean and SD from at least two independent experiments

The effects of these mutations are not nearly as severe as the PH domain deletion. However, a partial rescue is not unexpected, because these mutant PH domain retain 30% of the $PI(4,5)P_2$ binding capacity of the wild-type PH domain.

We also examined the effect of the R1496A mutation on the movement of UNC-104::GFP in neurites of cultured neurons. Our observations reveal that UNC-104_{R1496A}::GFP particles move at half the speed and with half the run length of wild-type UNC-104::GFP. This result is somewhat unexpected, because it indicates that a point mutant located distal from the motor domain can affect movement characteristics and not simply the number of membranes transported. Two explanations might account for this result. First, one might expect a reduction in velocity and run length if these parameters are proportional to the number of motors bound to the membrane and if motor binding to the cargo is reduced. This hypothesis might pertain if transport is generated by nonprocessive, monomeric UNC-104::GFP motors, where multiple motors might act cooperatively to transport a membrane cargo at maximal speed (Howard, 1997; Pierce *et al.*, 1999; Rogers *et al.*, 2001). UNC-104 behaves biochemically as a monomer in low concentrations in solutions (Pierce *et al.*, 1999) and physiological transport by monomeric KIF1A (the mouse orthologue of UNC-104) has been proposed (Okada and Hirokawa, 1999; Okada *et al.*, 2003). An alternative hypothesis is that UNC-104 can dimerize through a weak coiled-coil interaction in the neck domain when it becomes concentrated into $PI(4,5)P_2$-enriched lipid raft microdomains (Klopfenstein *et al.*, 2002). Once dimerized, UNC-104 becomes highly processive, and a single UNC-104 dimer can transport liposomes (Tomishige *et al.*, 2002). Moreover, in vitro studies have shown that membrane transport generated by a single dimeric UNC-104 occurs at 2–3-fold faster rates than that produced by multiple monomers (Tomishige *et al.*, 2002). According to this model, UNC-104_{R1496A}, with its weaker affinity for $PI(4,5)P_2$, may not be as effectively concentrated in lipid rafts and hence the equilibrium on the membrane surface may be shifted in favor of slower moving monomers vs. fast moving dimers. To distinguish between these possibilities, assays to detect the oligomeric state of UNC-104 on membranes will need to be developed.

Comparison of UNC-104–mediated Transport In Vitro and In Vivo

The conclusion that the PH domain serves a critical role in transport agrees with our previous results using bacterially expressed "mini-motors" (a shortened construct of the motor and PH domains joined directly to one another) and purified liposomes or membranes vesicles derived from *Dictyostelium* extracts. However, other findings differed between the prior in vitro study and this work in living worms (Klopfenstein *et al.*, 2002). First, substitution of the *Dicytostelium* PH domain with other PH domains (from PLCδ1 or from the dual adapter protein for phosphotyrosine and 3-phosphoinositide-1 [DAPPI]) resulted in reconstitution of movement in vitro, albeit with twofold reduced frequency and velocity. In contrast, in this study, we find that substitution of the *C. elegans* UNC-104 PH domain with the *Dictyostelium* UNC-104 PH domain or other lipid-binding modules produced only a very weak rescue of the *unc-104* phenotype. It is possible that this result reflects functions of

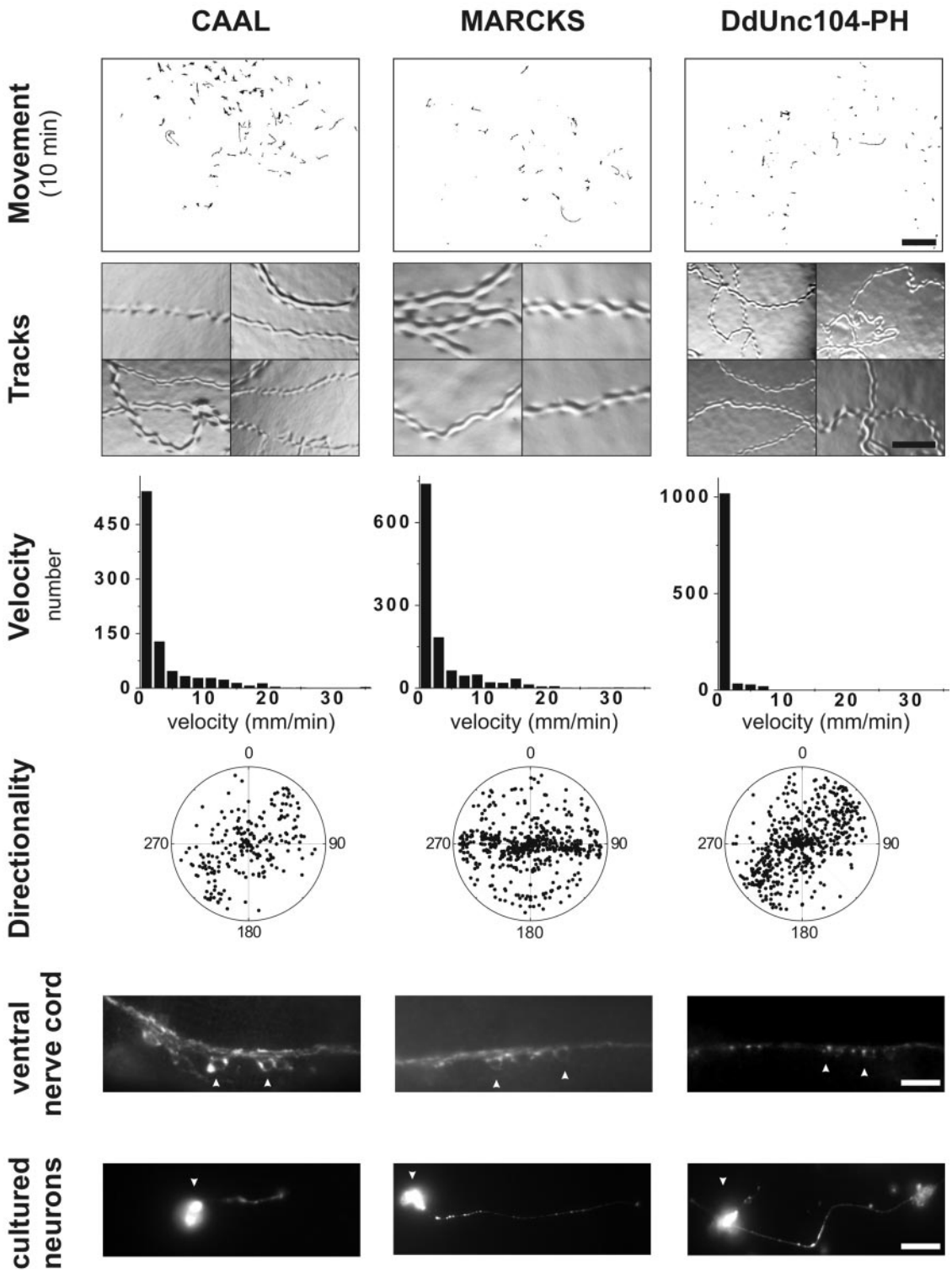

Figure 7. Substitutions of the UNC-104 PH domain with other lipid-binding modules only weakly or fails to rescue the *unc-104* phenotype. The movement of the transgenic worms (scale bar, 4.8 mm), agar tracks (scale bar, 0.13 mm), worm velocities, directional persistence, and analysis of synaptotagmin staining in the ventral nerve cord (scale bar, 10 μm) and in cultured neurons (scale bar, 10 μm) were performed as described in the legends to Figures 2–4. Cell body staining is indicated by the arrowheads. See text for description of phenotypes.

the PH domain other than PI(4,5)P_2 binding. Because PH domains are known to interact with proteins as well as lipids, binding of the *C. elegans* UNC-104 PH domain to specific protein partners may be particularly important for reconstitution of function in the setting of the nervous system as compared with in vitro assays.

Another intriguing difference between our previous in vitro studies with *Dictyostelium* Unc104 and this study in-

volves the long stalk region between the FHA and PH domain. Our in vitro studies showed that this stalk region could be deleted without impairing Unc104–mediated transport of liposomes or native *Dictyostelium* vesicles (Klopfenstein *et al.*, 2002). In contrast, similar deletions impaired the ability of the UNC-104 motor to rescue the *unc-104* phenotype, although the effects were less severe than the PH domain deletion (deletions shown in Figure 1 and data in Supplementary Figure 2). Although this region has no obvious structural motif or domain fold, it is conserved among Unc104/KIF1A kinesins from *Dictyostelium* to humans in overall length and sequence (sequence identity of ~50%, homology ~64%) as the PH domain (56% identity, 75% homology). Two hypotheses might account for the requirement of the stalk region in UNC-104–mediated transport in the *C. elegans* nervous system. One hypothesis is that the stalk serves as a spacer between the motor head and the cargo-binding domain. To orient the motor properly on the membrane, the PH domain may need to be separated by a flexible, unstructured linker so not to interfere with microtubule binding and movement. This may be particularly important in the context of the dense cytoskeletal network of the axon. A second hypothesis, not exclusive of the first, is that the spacer region serves as an interaction domain that might serve a regulatory function. This notion has been advanced by recent work showing that the stalk region of murine KIF1A binds to the scaffolding protein liprin-alpha in vitro and that the two proteins colocalize in vivo (Shin *et al.*, 2003). In addition, the stalk may modulate the fold-back negative regulatory interaction involving the FHA, as described by Lee *et al.* (2004).

C. elegans as a System for Dissecting Mechanisms of Motor-Cargo Interactions

Many interactions between kinesin motors and putative receptors/adapters have been described in mammalian systems. However, proving the physiological relevance of these interactions has been hindered by the lack of facile genetics. Among metazoans, *Drosophila* has proven a successful genetic system for identifying novel kinesin receptors involved in axonal transport (Bowman *et al.*, 2000), but structure-function analysis of motor-cargo interactions is difficult due to the relatively time consuming process of preparing transgenic fly lines. In this study, the relative ease and speed of preparing transgenic *C. elegans* has enabled us to analyze the phenotypes of many UNC-104 mutants. Similar strategies can be applied to other kinesin family members that have a *C. elegans* phenotype. For example, the motor Osm-3 (KIF17) (Signor *et al.*, 1999) is involved in intraflagellar transport in the specialized dendritic processes of chemosensory neurons. Rescue of chemosensory defects by expression of wild-type or mutant Osm-3 in an *osm-3* null background could be used to map cargo-binding sites for this motor. In addition, *C. elegans* provides an ideal system for understanding how changing motor output affects physiological function in vivo. For example, motor domain point mutants or chimeras could be generated that affect velocity, force, or processivity, and the properties of such motors could be tested in a physiological setting by introducing them in *unc-104* animals. Similarly, constitutive monomeric or dimeric UNC-104 constructs could be tested for in vivo function. Thus, *C. elegans* offers a tractable and powerful system for examining motor-driven transport by combining genetics with cell biological and biophysical investigations.

ACKNOWLEDGMENTS

We thank Drs. Mimi Zhou and Jon Scholey for the gift of Unc-104 construct, Dr. Kang Shen for experimental advice and help with nematode culturing, Dr. Nico Stuurman for developing the ImageJ tracking program, Dr. Jami Dantzker for introduction into neuronal cell culture, Dr. Mike Nonet for the gift of synaptotagmin antibody, and Dr. Cori Bargmann for stimulating discussions and encouraging us to begin work on this system. This work was supported by a fellowship from the Swiss National Science Foundation (823A-064692) to D.R.K. and National Institutes of Health Grant 38499 to R.D.V.

REFERENCES

Bowman, A.B., Kamal, A., Ritchings, B.W., Philp, A.V., McGrail, M., Gindhart, J.G., and Goldstein, L.S. (2000). Kinesin-dependent axonal transport is mediated by the sunday driver (SYD) protein. Cell *103,* 583–594.

Brenner, S. (1974). The genetics of Caenorhabditis elegans. Genetics *77,* 71–94.

Christensen, M., Estevez, A., Yin, X., Fox, R., Morrison, R., McDonnell, M., Gleason, C., Miller, D.M., 3rd, and Strange, K. (2002). A primary culture system for functional analysis of C. elegans neurons and muscle cells. Neuron *33,* 503–514.

Finney, M., and Ruvkun, G. (1990). The unc-86 gene product couples cell lineage and cell identity in C. elegans. Cell *63,* 895–905.

Fire, A. (1986). Integrative transformation of Caenorhabditis elegans. EMBO J. *5,* 2673–2680.

Hall, D.H., and Hedgecock, E.M. (1991). Kinesin-related gene unc-104 is required for axonal transport of synaptic vesicles in C. elegans. Cell *65,* 837–847.

Hirokawa, N., Noda, Y., and Okada, Y. (1998). Kinesin and dynein superfamily proteins in organelle transport and cell division. Curr. Opin. Cell Biol. *10,* 60–73.

Howard, J. (1997). Molecular motors: structural adaptations to cellular functions. Nature *389,* 561–567.

Kavran, J.M., Klein, D.E., Lee, A., Falasca, M., Isakoff, S.J., Solnik, E.Y., Lemmon, M.A. (1998). Specificity and promiscuity in phosphoinositide binding by pleckstrin homology domains. J. Biol. Chem. *273,* 30497–30508.

Klopfenstein, D.R., Tomishige, M., Stuurman, N., and Vale, R.D. (2002). Role of phosphatidylinositol(4,5)bisphosphate organization in membrane transport by the Unc104 kinesin motor. Cell *109,* 347–358.

Laux, T., Fukami, K., Thelen, M., Golub, T., Frey, D., and Caroni, P. (2000). GAP43, MARCKS, and CAP23 modulate PI(4,5)P(2) at plasmalemmal rafts, and regulate cell cortex actin dynamics through a common mechanism. J. Cell Biol. *149,* 1455–1472.

Lee J.R. Shin, H., Ko, J., Choi, J., Lee, H., Kim, E. (2003). Characterization of the movement of the kinesin motor KIF1A in living neurons. J. Biol. Chem. *278,* 2624–2629.

Lemmon, M.A. (2003). Phosphoinositide recognition domains. Traffic *4,* 201–213.

Lemmon, M.A., and Ferguson, K.M. (2001). Molecular determinants in pleckstrin homology domains that allow specific recognition of phosphoinositides. Biochem. Soc. Trans. *29,* 377–384.

Mello, C.C., Kramer, J.M., Stinchcomb, D., and Ambros, V. (1991). Efficient gene transfer in C. elegans: extrachromosomal maintenance and integration of transforming sequences. EMBO J. *10,* 3959–3970.

Miki, H., Setou, M., Kaneshiro, K., and Hirokawa, N. (2001). All kinesin superfamily protein, KIF, genes in mouse and human. Proc. Natl. Acad. Sci. USA *98,* 7004–7011.

Muresan, V. (2000). One axon, many kinesins: what's the logic? J. Neurocytol. *29,* 799–818.

Nonet, M.L., Grundahl, K., Meyer, B.J., and Rand, J.B. (1993). Synaptic function is impaired but not eliminated in C. elegans mutants lacking synaptotagmin. Cell *73,* 1291–1305.

Okada, Y., Higuchi, H., and Hirokawa, N. (2003). Processivity of the single-headed kinesin KIF1A through biased binding to tubulin. Nature *424,* 574–577.

Okada, Y., and Hirokawa, N. (1999). A processive single-headed motor: kinesin superfamily protein KIF1A. Science *283,* 1152–1157.

Okada, Y., and Hirokawa, N. (2000). Mechanism of the single-headed processivity: diffusional anchoring between the K-loop of kinesin and the C terminus of tubulin. Proc. Natl. Acad. Sci. USA *97,* 640–645.

Okada, Y., Yamazaki, H., Sekine-Aizawa, Y., and Hirokawa, N. (1995). The neuron-specific kinesin superfamily protein KIF1A is a unique monomeric

motor for anterograde axonal transport of synaptic vesicle precursors. Cell *81,* 769–780.

Otsuka, A.J., Jeyaprakash, A., Garcia-Anoveros, J., Tang, L.Z., Fisk, G., Hartshorne, T., Franco, R., and Born, T. (1991). The C. elegans unc-104 gene encodes a putative kinesin heavy chain-like protein. Neuron *6,* 113–122.

Pierce, D.W., Hom-Booher, N., Otsuka, A.J., and Vale, R.D. (1999). Single-molecule behavior of monomeric and heteromeric kinesins. Biochemistry *38,* 5412–5421.

Pollock, N., de Hostos, E.L., Turck, C.W., and Vale, R.D. (1999). Reconstitution of membrane transport powered by a novel dimeric kinesin motor of the Unc104/KIF1A family purified from Dictyostelium. J. Cell Biol. *147,* 493–506.

Reid, E. *et al.* (2002). A kinesin heavy chain (KIF5A) mutation in hereditary spastic paraplegia (spg10). Am. J. Hum. Genet. *71,* 1189–1194.

Rogers, K.R., Weiss, S., Crevel, I., Brophy, P.J., Geeves, M., and Cross, R. (2001). KIF1D is a fast non-processive kinesin that demonstrates novel K-loop-dependent mechanochemistry. EMBO J. *20,* 5101–5113.

Shin, H. *et al.* (2003). Association of the kinesin motor KIF1A with the multimodular protein liprin-alpha. J. Biol. Chem. *278,* 11393–11401.

Signor, D., Wedaman, K.P., Rose, L.S., and Scholey, J.M. (1999). Two heteromeric kinesin complexes in chemosensory neurons and sensory cilia of Caenorhabditis elegans. Mol. Biol. Cell *10,* 345–360.

Tomishige, M., Klopfenstein, D.R., and Vale, R.D. (2002). Conversion of Unc104/KIF1A kinesin into a processive motor after dimerization. Science *297,* 2263–2267.

Vale, R.D. (2003). The molecular motor toolbox for intracellular transport. Cell *112,* 467–480.

Wang, J., Gambhir, A., Hangyas-Mihalyne, G., Murray, D., Golebiewska, U., and McLaughlin, S. (2002). Lateral sequestration of phosphatidylinositol 4,5-bisphosphate by the basic effector domain of myristoylated alanine-rich C kinase substrate is due to nonspecific electrostatic interactions. J. Biol. Chem. *277,* 34401–34412.

Yonekawa, Y., Harada, A., Okada, Y., Funakoshi, T., Kanai, Y., Takei, Y., Terada, S., Noda, T., and Hirokawa, N. (1998). Defect in synaptic vesicle precursor transport and neuronal cell death in KIF1A motor protein-deficient mice. J. Cell Biol. *141,* 431–441.

Zhao, C. *et al.* (2001). Charcot-Marie-Tooth disease type 2A caused by mutation in a microtubule motor KIF1Bbeta. Cell *105,* 587–597.

Zhou, H.M., Brust-Mascher, I., and Scholey, J.M. (2001). Direct visualization of the movement of the monomeric axonal transport motor UNC-104 along neuronal processes in living Caenorhabditis elegans. J. Neurosci. *21,* 3749–3755.